The Journal of Chemical Physics

Relationship between aged and vapor-deposited organic glasses: Secondary relaxations in methyl-*m*-toluate

Cite as: J. Chem. Phys. **151**, 144502 (2019); https://doi.org/10.1063/1.5123305
Submitted: 06 August 2019 . Accepted: 19 September 2019 . Published Online: 08 October 2019

B. J. Kasting, M. S. Beasley, A. Guiseppi-Elie, R. Richert, and M. D. Ediger

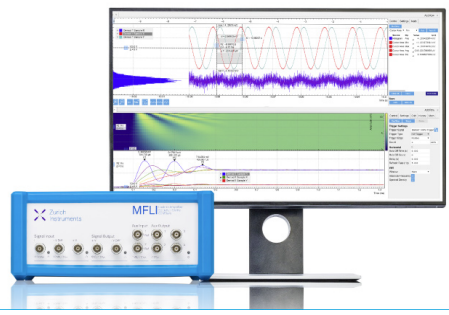

The Journal of Chemical Physics ARTICLE scitation.org/journal/jcp

Relationship between aged and vapor-deposited organic glasses: Secondary relaxations in methyl-*m*-toluate

Cite as: J. Chem. Phys. 151, 144502 (2019); doi: 10.1063/1.5123305
Submitted: 6 August 2019 • Accepted: 19 September 2019 •
Published Online: 8 October 2019

B. J. Kasting,[1,a)] M. S. Beasley,[1] A. Guiseppi-Elie,[2] R. Richert,[3] and M. D. Ediger[1]

AFFILIATIONS

[1] Department of Chemistry, University of Wisconsin – Madison, Madison, Wisconsin 53706, USA
[2] Department of Biomedical Engineering, Texas A&M University, College Station, Texas 77843, USA
[3] Department of Chemistry and Biochemistry, Arizona State University, Tempe, Arizona 85287, USA

[a)] **Author to whom correspondence should be addressed:** bkasting@wisc.edu

ABSTRACT

In situ interdigitated electrode broadband dielectric spectroscopy was used to characterize the excess wing relaxations in vapor-deposited and aged glasses of methyl-*m*-toluate (MMT, T_g = 170 K). MMT displays typical excess wing relaxations in dielectric spectra of its supercooled liquid and glasses. Physical vapor deposition produced glasses with degrees of suppression of the excess wing relaxation that varied systematically with deposition conditions, up to a maximum suppression of more than a factor of 3. The glass deposited at a relatively high temperature, 0.96 T_g (163 K), showed the same amount of suppression as that of a liquid-cooled glass aged to equilibrium at this temperature. The suppression of the excess wing relaxation was strongly correlated with the kinetic stability of the vapor-deposited glasses. Comparisons with aged MMT glasses allowed an estimate of the structural relaxation time of the vapor-deposited glasses. The dependence of the estimated structural relaxation times upon the substrate temperature was found to be stronger than Arrhenius but weaker than Vogel-Fulcher-Tammann dependence predicted from extrapolation of relaxation times in the supercooled liquid. Additionally, this work provides the first example of the separation of primary and secondary relaxations using physical vapor deposition.

I. INTRODUCTION

As a liquid is supercooled below its melting temperature, its viscosity and structural relaxation time increase dramatically. When the structural relaxation time increases beyond approximately 100 s, the material becomes a glass at the glass transition temperature, T_g. Although the large-scale structure of the material becomes practically fixed below T_g, molecular relaxations do not stop in the glassy state and these continued motions are generically known as secondary relaxations.[1] Secondary relaxations are of interest for several reasons. They can provide insight into features of the amorphous region of the potential energy landscape.[2,3] Among the various types of secondary relaxations, the Johari-Goldstein (JG) relaxation is the most fundamental as it involves motion of the entire molecule as a precursor to the structural relaxation.[4] The study of secondary relaxations extends beyond fundamental questions in glass physics. It has been reported that freezing out the secondary relaxations of amorphous pharmaceuticals increases the stability of the amorphous state with respect to crystallization.[5] Control of secondary relaxations may also have applications in quantum computing because minimization of motion at very low temperature can improve the coherence time of qubits.[6]

Secondary relaxations can be categorized based upon their manifestation in the dielectric relaxation spectra.[7] Secondary relaxations can appear either as a well-separated β peak distinct from the α peak (associated with the glass transition) or as a gradual decrease in the slope on the high frequency flank of the α peak. This second scenario is often called an excess wing relaxation and it can be described empirically as the sum of two peaks that are not separated, but it has been debated whether this empirical description is fundamentally correct.[8] Evidence in favor of the submerged peak interpretation of the excess wing has been provided by aging[9,10] and

pressure densification experiments[11] on various materials. In these experiments, the excess wing was shown to develop into a more distinct shoulder because the α peak reacts more strongly to changes in temperature or pressure than the submerged β peak. Secondary relaxations can also be characterized based upon their molecular origin, with those originating from motion of the entire molecule known as Johari-Goldstein (JG) relaxation.[12] Unambiguous determination of the molecular origin of a secondary relaxation may be difficult and may require multidimensional nuclear magnetic resonance (NMR) experiments on selectively deuterated samples.[13,14] Ngai and Paluch developed a set of criteria to allow one to classify secondary relaxations based on their dynamic properties in response to changes in temperature and pressure.[11]

Physical vapor deposition (PVD) can be used to modify the physical and dynamic properties of a glass, including secondary relaxation processes. During PVD, molecules are evaporated onto a temperature-controlled substrate. Molecules at the free surface of the growing film have greater mobility than molecules in the bulk.[15] For the surface equilibration mechanism,[16,17] this mobile surface layer is the origin of the unique properties of vapor-deposited glasses because it allows molecules to efficiently sample the energy landscape and find low energy configurations even below T_g. The two main control parameters in PVD are the substrate temperature and the deposition rate. Lowering the substrate temperature reduces the thickness of the mobile surface layer and the inherent mobility of molecules. The deposition rate controls the surface residence time, i.e., how long a molecule spends on the free surface before being buried by further deposition. The effects of substrate temperature and deposition rate combine to modify glass properties like density, kinetic stability, and secondary relaxation amplitude. For example, relative to a liquid-cooled (LC) glass, PVD glasses can be up to 1.3% more dense[18] and, during isothermal annealing above T_g, this higher density is associated with an increased lifetime of a glass by a factor of up to 10^5.[16]

There have been several previous studies of secondary relaxation processes in vapor-deposited glasses and, in each case, the amplitude of the secondary process is suppressed relative to the corresponding liquid-cooled glass.[19–22] We understand this to mean that the tighter packing of PVD glasses restricts the amplitude of the molecular motions associated with secondary relaxations. The first report of PVD being used to prepare glasses with suppressed secondary relaxations showed that the β relaxation of toluene could be reduced by as much as 70% under optimal deposition conditions.[19] Rodríguez-Tinoco *et al.* characterized the secondary relaxation of additional PVD glasses; these systems showed a range of suppression from 26% to 89% for glasses deposited at 0.85 T_g.[21] A summary of secondary relaxation suppression in vapor-deposited glasses can be found in Fig. 1. It appears that suppression of the secondary relaxation by 70%–80% is a quite common feature of these systems. For some systems, it has been observed that the relaxation time associated with the secondary relaxation is also altered in PVD glasses. Shifts have been reported to both longer and shorter times,[21] and in all cases, the changes are less than one order of magnitude. For Johari-Goldstein relaxations, experimental evidence shows that the change in secondary relaxation time due to changes in glass density is restricted to approximately 1 decade.[23]

Here, we perform *in situ* broadband dielectric spectroscopy on vapor-deposited and liquid-cooled glasses of methyl-*m*-toluate (MMT) in order to study the suppression of the secondary relaxation and connect the properties of aged and vapor-deposited glasses. The supercooled liquid state of MMT has been well-characterized by broadband dielectric spectroscopy.[24] The effect of physical vapor deposition on the kinetic stability of MMT glasses has been studied by AC nanocalorimetry[25] and interdigitated electrode broadband dielectric spectroscopy.[26] In contrast to most previous studies of secondary relaxations in vapor-deposited glasses,[19–21] the secondary relaxation in MMT is not well-separated from the α peak.[24]

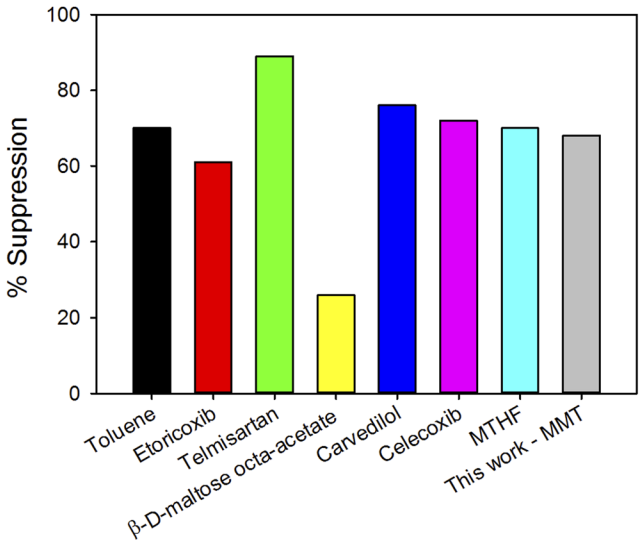

FIG. 1. Secondary relaxation suppression observed in organic glasses when vapor-deposited near 0.85 T_g. Toluene,[19] Etoricoxib,[20] Telmisartan,[21] β-D-maltose octa-acetate,[21] Carvedilol,[21] Celecoxib,[21] and MTHF.[22]

We find that secondary relaxations in vapor-deposited glasses of MMT are suppressed at all deposition temperatures below T_g, with a maximum suppression of approximately 70%. We find a strong correlation between the suppression of secondary relaxations in MMT and the kinetic stability of the vapor-deposited glasses. By comparing the secondary relaxation process in both vapor-deposited and aged liquid-cooled glasses, we present a method for estimating the structural relaxation time τ_α of vapor-deposited glasses. The dependence of the estimated structural relaxation times upon the substrate temperature was found to be stronger than Arrhenius but weaker than Vogel-Fulcher-Tammann (VFT) dependence predicted from extrapolation of relaxation times in the supercooled liquid. Finally, for MMT, we show that PVD can be used to resolve the excess wing secondary relaxation into a β relaxation peak and is a much more efficient method for achieving this separation than is physical aging.

II. EXPERIMENTAL

Methyl-*m*-toluate (MMT, 98%, T_g = 170 K) was purchased from Alfa Aesar and used as received. Vapor-deposited glasses were prepared in a custom-built vacuum chamber with a base pressure $<10^{-7}$ Pa. Material was introduced into the chamber from a

stainless-steel reservoir through a fine leak valve. The temperature of the interdigitated electrode device which served as our substrate was set by heating against a cold cup filled with liquid nitrogen. Absolute temperature was calibrated based on the α relaxation time measured in the supercooled liquid. This relaxation time was compared to literature data, and a temperature offset was obtained (typically 5–7 K). Deposition rate was monitored by the chamber pressure as indicated by the ionization gauge. The typical deposition pressure was 2×10^{-4} Pa which corresponds to a deposition rate of ~0.2 nm/s. Film thicknesses were approximately 1.3 μm. The interdigitated electrode device, Abtech IME 1025.3-FD-Pt-U, was made of borosilicate glass with two pairs of platinum electrodes microlithographically patterned (lift off) on the surface. Each pair of interdigitated electrodes consisted of 50 fingers, each 10 μm wide, with a 10 μm serpentine gap between the fingers. One pair of electrodes was open to vapor deposition while the other pair of electrodes was covered, serving as a reference measurement of the device response. A common oscillating voltage was applied to both electrodes from a Solartron SI 1260 impedance analyzer. The differential impedance signal is then converted to dielectric permittivity as described previously.[27] As a check on our procedures, we verified that the dielectric relaxation spectra of the supercooled liquid and liquid-cooled glasses of MMT collected on the interdigitated electrode device were consistent with spectra reported previously, using a parallel plate capacitor.[24]

Two types of experiments were performed on glasses of MMT. In the first set of experiments, isothermal dielectric loss spectra of a vapor-deposited or aged glass were collected at a series of measurement temperatures below T_g (170 K), wherein the measurement temperature was increased from low to high. Data were collected in the frequency range 10^{-1}–10^5 Hz with 8 points per decade. The film was then heated to a temperature above T_g and held until the spectrum of the α peak stopped evolving, indicating that the supercooled liquid state had been attained. The film was then cooled at 5 K/min to the lowest temperature used for the measurements on the vapor-deposited or aged glass. The sequence of measurements was then repeated on the unaged liquid-cooled glass, utilizing the same measurement temperatures.

Isothermal dielectric spectra were analyzed on the assumption that the excess wing is caused by a β peak that is not well-separated from the α peak. Spectra were fit to the sum of the Havriliak-Negami function to represent the α peak and the Cole-Cole function to represent the β peak, Eq. (1). The parameters τ_{HN}, τ_{CC}, and $\Delta\varepsilon_{CC}$ were determined by fitting. The other four parameters were fixed to values obtained from unconstrained fits to dielectric data of the supercooled liquid of MMT,[24] since these values are essentially constant near T_g. Thus, we assume that time-temperature superposition applies separately for the α and β processes near T_g,

$$\varepsilon^*(f) = \varepsilon_\infty + \frac{\Delta\varepsilon_{HN}}{\left(1 + (2\pi i f \tau_{HN})^\alpha\right)^\gamma} + \frac{\Delta\varepsilon_{CC}}{1 + (2\pi i f \tau_{CC})^\beta}. \quad (1)$$

In Fig. 7 below, we show τ_α values obtained from these fits; for this figure, $\tau_\alpha = \tau_{HN}$.

The second type of experiment performed on MMT glasses involved ramping the temperature at a constant rate of 5 K/min while measuring the dielectric loss at a fixed frequency of 20 Hz. These experiments allowed quantification of the kinetic stability of vapor-deposited and aged glasses. The samples were then heated to T_g + 20 K and held at this temperature for 5 min to complete the conversion to the supercooled liquid, and then cooled at 5 K/min to 144 K. Two additional heating and cooling runs were performed (without the isothermal step at T_g + 20 K) to measure the response of the unaged liquid-cooled glass. The onset temperatures for vapor-deposited and aged glasses were determined from the intersection of tangent lines drawn to the glassy behavior and the initial slope of the α peak (illustrated below in Fig. 3).

III. RESULTS

A. Isothermal dielectric relaxation spectra

Isothermal dielectric relaxation spectra were collected to quantify the effect of physical vapor deposition and the aging of liquid-cooled glasses on the amplitude of the secondary relaxation and the separation between the primary and secondary relaxations. The dielectric loss spectra for a glass deposited at 0.84 T_g (143 K) and a liquid-cooled glass are compared in Fig. 2 as a representative example of the differences between vapor-deposited and liquid-cooled glasses. In the spectrum of the liquid-cooled glass, one can see the excess wing behavior with no separation between the primary and the secondary relaxations; this spectrum can be described as a gradual change from a relatively steep negative slope to a shallower negative slope with increasing frequency. In contrast, the glass vapor-deposited at 0.84 T_g (143 K) displays a region of near zero slope between two regions of the negative slope. The separation of spectral features as a result of vapor deposition is quite similar to that observed when glycerol is aged for one month.[9]

In Fig. 2, the amplitude of the secondary relaxation has been reduced by approximately 70% (more than a factor of 3) for the vapor-deposited glass relative to that of the liquid-cooled glass. Additionally, the α peak in the vapor-deposited glass has been shifted

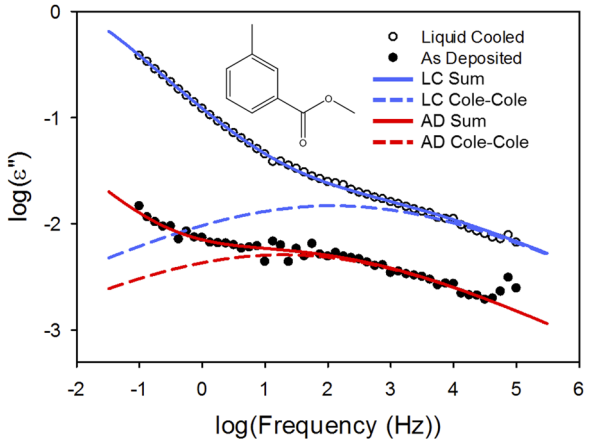

FIG. 2. Dielectric loss as a function of frequency for a liquid-cooled (LC) and an as-deposited (AD) glass of MMT. The vapor-deposited sample was deposited at 0.84 T_g (143 K). Both samples were measured at 170 K (T_g). Solid lines are the fits to Eq. (1) and dashed lines show the contribution of the secondary process to the overall fit. The amplitude of the secondary relaxation process is suppressed by 68% in the vapor-deposited glass. The structure of MMT is shown in the inset.

approximately three decades toward lower frequencies based on fits of the spectrum to Eq. (1). The spectrum for the vapor-deposited glass could also be interpreted as a decrease in the amplitude of the α process without a change in the relaxation time. We reject this interpretation for two reasons. First, the amplitude of the α peak is nearly constant in the supercooled liquid, independent of temperature. Second, this interpretation would be inconsistent with the long isothermal transformation times of the vapor-deposited glass (see below).[25,26] Although it has been shown that physical vapor deposition can affect the characteristic time scale of secondary relaxations,[19–21] we make no attempt to quantify changes in the time scale of secondary relaxations in vapor-deposited glasses of MMT relative to their liquid-cooled counterparts due to their breadth and lack of separation from the α peak.

Experiments similar to Fig. 2 were performed on glasses vapor-deposited at many substrate temperatures and also on liquid-cooled glasses aged for various periods. The results are collected and discussed below.

B. Temperature ramping experiments

Temperature-ramping experiments were performed to characterize the kinetic stability of the vapor-deposited glasses. Figure 3 shows a representative temperature ramping experiment utilizing the dielectric response at 20 Hz. The primary feature of these experiments is the increased onset temperature observed in the first scan. The onset temperature is the temperature at which the glass begins to transform into the supercooled liquid. The onset temperature of kinetically stable glasses will be greater than the onset temperature of a freshly prepared liquid-cooled glass. Aging a liquid-cooled glass is one way to increase kinetic stability, but PVD is a much more efficient method to prepare kinetically stable glasses.[28] The onset temperature was measured with a heating rate of 5 K/min to allow for comparison to AC nanocalorimetry measurements of vapor-deposited glasses of MMT.[25] The kinetic stability results from the current work agree with the previously published results within the experimental error (Fig. S1).

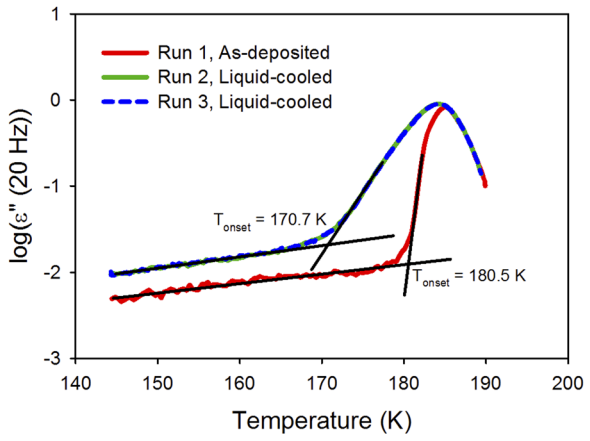

FIG. 3. Dielectric loss at 20 Hz as a function of temperature for a vapor-deposited glass of MMT. Run 1, dielectric loss upon heating an MMT glass prepared by vapor deposition at 0.90 T_g (153 K). Runs 2 and 3, dielectric loss upon heating liquid-cooled MMT glass prepared from the transformed vapor-deposited glass. Heating and cooling rates are 5 K/min. The greater onset temperature and lower initial amplitude of run 1 relative to runs 2 and 3 are indicative of a kinetically stable glass with suppressed secondary relaxations.

A second feature of these experiments is the diminished loss in the vapor-deposited glass prior to its transformation in the supercooled liquid. This is the signature of the secondary relaxation suppression, measured at a fixed frequency as a function of temperature. The results of experiments like those shown in Fig. 3 are collected and discussed below.

C. Aging experiments on liquid-cooled glasses

Aging experiments were performed on liquid-cooled glasses at three annealing temperatures to compare glasses annealed at a particular temperature to glasses vapor-deposited at that same temperature. Figure 4(a) shows the dielectric relaxation spectra of liquid-cooled MMT glass before and after annealing at 0.96 T_g (163 K) for 20 h, in comparison with MMT vapor-deposited at 0.95 T_g (161 K). The spectra have been normalized by the amplitude of the α peak subsequently observed in the supercooled liquid state to correct for small differences in the film thickness. In Fig. 4(a), we observe a good overlap of the vapor-deposited glass spectrum with the spectrum of the liquid-cooled glass that has been annealed to equilibrium at 0.96 T_g (163 K). This provides evidence that vapor-deposited glasses can reproduce the dynamical properties expected for the supercooled liquid below T_g. Further evidence to this point is provided in Fig. 5(a) which shows the decrease in the secondary relaxation amplitude that took place during aging. For all aging experiments, shown below in Fig. 5, the decrease of the secondary relaxation amplitude was obtained by multiplying ε'' by a shift factor to overlap the excess wing region of the spectrum with the excess wing region of the initial spectrum. This procedure yielded estimates of the suppression with less impact from experimental noise. The amplitude of the secondary relaxation process for the liquid-cooled glass decreased smoothly during aging until reaching equilibrium at $10^{4.4}$ s. The dashed line in Fig. 5(a) shows the value of the secondary relaxation suppression expected for a glass vapor-deposited at 0.96 T_g (163 K). This value was obtained by interpolation of data obtained from nearby substrate temperatures, and the estimated error in the interpolation is indicated by the error bar on the horizontal line. Within the error, the equilibrium amplitude of the secondary relaxation agrees with that achieved by vapor deposition.

Similarly, we performed experiments to compare vapor-deposited and aging liquid-cooled glasses at 0.92 T_g (156 K). This temperature was chosen based on the observation that, for other systems, for substrate temperatures somewhat below T_g, vapor-deposited glasses have the properties expected for glasses prepared from deeply supercooled liquids.[29–31] This equivalence can be interpreted as meaning physical vapor deposition allows for efficient equilibration of the growing film. This result was first shown for the enthalpy of vapor-deposited ethylbenzene by adiabatic calorimetry.[29] Recently, Beasley *et al.* demonstrated that the density and refractive index of vapor-deposited ethylbenzene glasses also follow the extrapolated supercooled liquid behavior down to 0.89 T_g (103 K).[30]

Figure 4(b) shows that annealing a liquid-cooled glass at 0.92 T_g (156 K) for 20 h achieves similar levels of suppression to those

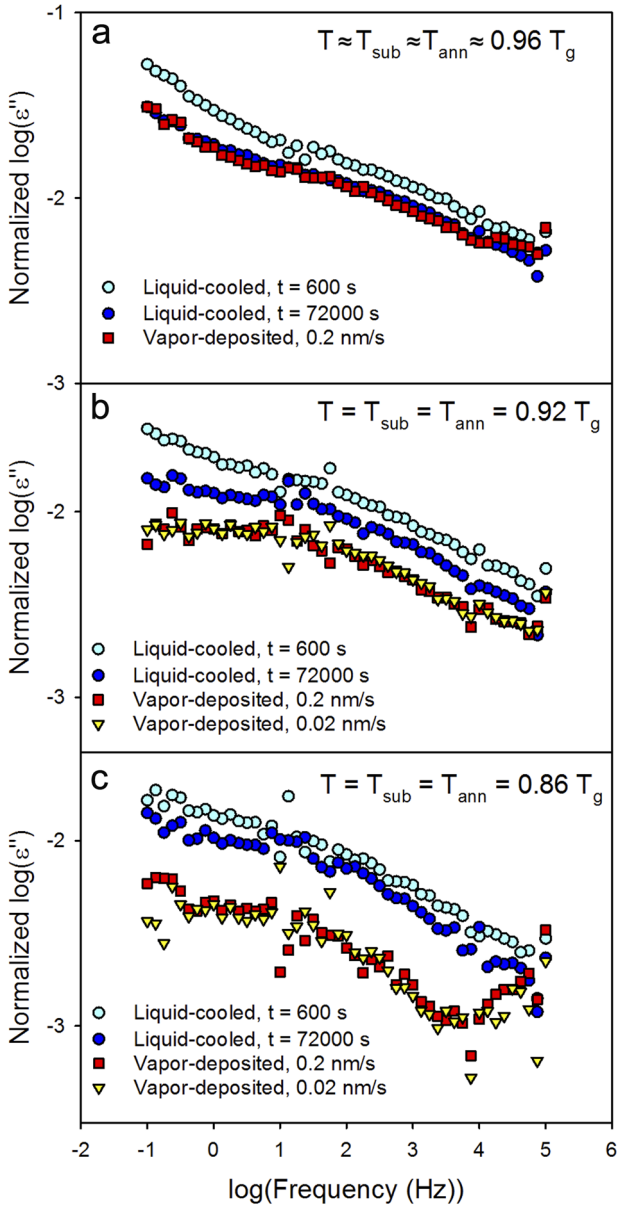

FIG. 4. Comparison of dielectric loss spectra of aged and vapor-deposited glasses of MMT. The upper spectrum (light blue circles) in each panel is the liquid-cooled glass before annealing at the temperature (T_{ann}) indicated in the panel. The bottom spectra (red squares and yellow triangles) are glasses vapor-deposited at the substrate temperature (T_{sub}) indicated in the panel. Liquid-cooled glasses annealed for 20 h (dark blue circles) have the same dielectric response as the vapor-deposited glass at the highest temperature, panel (a), but show much less suppression of the secondary relaxation process at lower temperatures, panels (b) and (c). In panels (b) and (c), there is no significant difference between the spectra of glasses deposited at 0.2 nm/s and 0.02 nm/s.

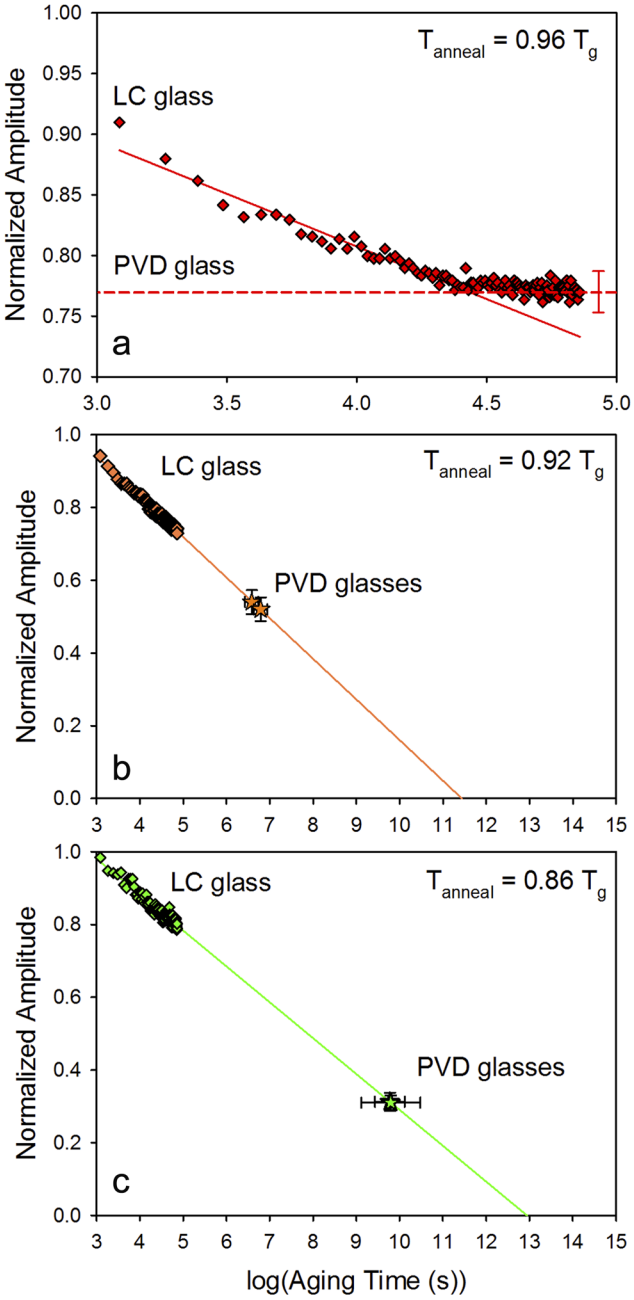

FIG. 5. Secondary relaxation amplitude as a function of aging time for liquid-cooled glasses annealed at the temperature indicated in the panel, with comparisons to vapor-deposited glasses. Panel (a): The solid line is a fit to the first 40 time points. The dashed line is the interpolated secondary relaxation amplitude for a glass of MMT vapor-deposited at 0.96 T_g (163 K) and 0.2 nm/s. The change of the slope in the aging data at ~$10^{4.4}$ s indicates that the sample aged to equilibrium. Panels (b) and (c): The solid line is an extrapolation of the aging data to zero amplitude. Vapor-deposited glasses (stars) were placed on the extrapolation to estimate the equivalent age of the samples. Vertical error bars represent the standard deviation of multiple measurements. Horizontal error bars represent the range of estimated times arising from the uncertainty of the slope and intercept from the linear regression.

achieved during aging at 0.96 T_g (163 K). However, the vapor-deposited glasses prepared at 0.92 T_g (156 K) have a significantly lower secondary relaxation amplitude than that achieved by aging the liquid-cooled glass for 20 h, even though these films required

only about 2 h of deposition (0.2 nm/s). We performed an additional deposition at 0.02 nm/s to check if increasing the surface residence time would allow for more secondary relaxation suppression. As shown in Fig. 4(b), lowering the deposition rate by one order of magnitude did not lead to a further decrease in the secondary relaxation strength, within the experimental error. The solid line in Fig. 5(b) shows the extrapolation of the aging experiment on the liquid-cooled glass to long times. The PVD glasses have been placed on this line as an estimate of the equivalent age of the vapor-deposited glasses, as discussed below.

Finally, we performed experiments to compare vapor-deposited and aging liquid-cooled glasses at 0.86 T_g (146 K). At this temperature, we observe very little decrease in the amplitude of secondary relaxations in the liquid-cooled glass after 20 h of aging, as shown in Fig. 4(c). As was the case for 0.92 T_g (156 K), the glasses vapor-deposited at 0.86 T_g (146 K) show a much lower amplitude of secondary relaxations than the aged liquid-cooled glasses; the glasses deposited at 0.86 T_g (146 K) have an even lower amplitude than the glasses deposited at 0.92 T_g (156 K). The overlap of the two vapor-deposited spectra in Fig. 4(c) indicates that lowering the deposition rate by an order of magnitude did not change the observed suppression of the secondary relaxation. We again estimate the equivalent age of the vapor-deposited glasses by placing the secondary relaxation suppression on the extrapolated aging line, Fig. 5(c).

The experiments shown in Figs. 4 and 5 are similar to physical aging experiments on glycerol and propylene carbonate that have previously been used to resolve excess wing secondary relaxations into clear shoulders.[9,10] This strategy is effective because the primary (α) and secondary relaxation times display a different sensitivity to the structural changes that occur during aging, with the primary process slowing down much more significantly as the sample equilibrates. These are demanding experiments that required a month of isothermal aging. Furthermore, for other systems, the separation that can be achieved by this approach may not be adequate to resolve the excess wing. Since PVD glasses can be considered to be "super-aged" in the as-prepared state,[29,30] it is reasonable to imagine that PVD might be even more effective in separating primary and secondary relaxations, in comparison to aging a liquid-cooled glass. This is apparent in Fig. 4(b) where we see the dielectric loss spectrum evolves from the liquid-cooled glass with a negative slope at all points to the vapor-deposited glasses with an approximately zero slope at low frequencies.

D. Correlation between kinetic stability and suppression of secondary relaxation

Figure 6 summarizes the results obtained from isothermal dielectric relaxation spectra and temperature ramping experiments for vapor-deposited and liquid-cooled glasses aged for 20 h. For the vapor-deposited glasses, the two sets of red points (solid and open squares) show a strong correlation between the suppression of the secondary relaxation and the kinetic stability, as a function of the substrate temperature during deposition. The suppression of secondary relaxations is defined as follows: The "peak" frequency of the secondary relaxation is determined from the fit parameters using $f_{peak} = \frac{1}{2\pi\tau_{CC}}$. The suppression of the secondary relaxation is then calculated from the ratio of the Cole-Cole peak amplitudes [denoted as $CC(f_{peak})$] obtained from the fits to Eq. (1) of the vapor-deposited and liquid-cooled glasses evaluated at their respective values of f_{peak}, Eq. (2),

$$\text{Suppression} = \left(1 - CC\left(f_{peak}\right)_{AD}/CC\left(f_{peak}\right)_{LC}\right). \quad (2)$$

For liquid-cooled glasses aged for 20 h, the data are consistent with a correlation between the suppression of the secondary relaxation and the kinetic stability, as seen by comparing the two sets of blue points (solid and open circles). The difference between the red points and blue points (solid and open circles) shows that physical vapor deposition is more efficient than aging at preparing glasses with highly suppressed secondary relaxations and increased onset temperature.

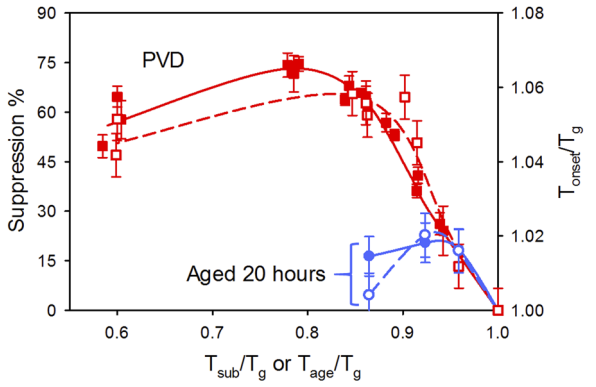

FIG. 6. Suppression of secondary relaxation and kinetic stability of vapor-deposited and aged liquid-cooled glasses, as a function of substrate temperature or aging temperature scaled by T_g = 170 K. Red and blue symbols/lines refer to vapor-deposited glasses and liquid-cooled glasses aged for 20 h, respectively. Filled and open symbols/lines refer to the left and right axes, respectively. Error bars for solid symbols represent the standard deviation of replicate measurements. Error bars for open symbols represent an estimate of the uncertainty in the tangent lines shown in Fig. 3.

IV. DISCUSSION

A. General features of the experimental data

In Fig. 6, we observe a good correlation between the suppression of the secondary relaxation and kinetic stability (as measured by T_{onset}/T_g) for vapor-deposited glasses of MMT. As the deposition temperature is lowered from T_g to 0.85 T_g, the suppression and kinetic stability both increase roughly linearly. Down to 0.96 T_g, the data for PVD and aged glasses overlap. The shape of the suppression and kinetic stability curves shown in Fig. 6 bear qualitative similarities to the density data of other vapor-deposited glasses.[18,32] The density of vapor-deposited glasses relative to liquid-cooled glasses also increases approximately linearly as the substrate temperature is lowered below T_g, and the density reaches a maximum near 0.80–0.85 T_g. All of these observations are qualitatively consistent with the surface equilibration mechanism[16,17] for PVD glass formation. Enhanced surface mobility allows equilibration during deposition at temperatures somewhat below the conventional T_g. At sufficiently low substrate temperatures, the surface mobility is so low that minimal equilibration occurs. The maximum impact of equilibration is observed at an intermediate substrate temperature, empirically found to be near 0.85 T_g. As a typical liquid-cooled glass is aged

toward equilibrium, it becomes more dense and more kinetically stable and exhibits suppressed secondary relaxations. From this perspective, it is natural that these three quantities show strong correlations in glasses prepared by vapor deposition.

In particular, the similar behavior of the density and secondary relaxation suppression as a function of substrate temperature is rationalized because tighter packing associated with the low temperature supercooled liquid would be expected to suppress the ability of the molecules to make small adjustments in their positions. In the case of liquid-cooled toluene glasses, NMR studies showed that the β peak could be modeled by the majority of molecules reorienting within cones with an angle of <10° and a small fraction with angles of 40° and 50°.[13,14] The suppression of the β peak in vapor-deposited glasses of toluene could be caused by a uniform reduction in these cone angles or by elimination of the largest angles.[19] The motion of MMT molecules is likely hindered similarly to toluene, although the molecular motion associated with the secondary relaxation in MMT is not yet known.

The results of secondary relaxation suppression and kinetic stability in vapor-deposited glasses of MMT allow for inferences about the potential energy landscape of this system. The potential energy landscape is commonly envisioned to be composed of metabasins, with transitions between metabasins being associated with structural relaxation. Within these metabasins exist smaller basins separated by lower barriers; transitions between these basins are associated with the secondary relaxation. The concurrent appearance of suppressed secondary relaxations and kinetic stability in these glasses imply that, deeper in the energy landscape, the metabasins are narrower and the barriers between metabasins are higher. Our observations also suggest that the barriers between basins, associated with the secondary relaxation, are not significantly different in vapor-deposited and liquid-cooled glasses. Testing the generality of these observations is an important area of investigation.

From the surface equilibration mechanism, we expect that at a fixed substrate temperature, glasses deposited at lower rates should be more equilibrated, unless equilibrium has already been achieved with the higher rate.[30] For glasses deposited at 0.92 T_g (156 K) and 0.86 T_g (146 K), we did not observe significant differences (relative to experimental error) in the amount of suppression or kinetic stability when the deposition rate was lowered from 0.2 nm/s to 0.02 nm/s and therefore make no deposition rate distinction in Fig. 6. (See the supplementary material for a version of this figure that distinguishes deposition rates.) While this observation would be consistent with the idea that these depositions produce the equilibrium supercooled liquid at these temperatures, the data are also consistent with the view that the experimental errors are large enough to obscure an important impact of the deposition rate. Given our results, even slower deposition at a given substrate temperature might succeed in preparing glasses with higher kinetic stability and a greater suppression of the secondary relaxation. Thus, in the discussion below, we describe the as-deposited films as glasses (and opposed to supercooled liquids).

It has been suggested that the suppression of secondary relaxations might be the cause of the reduced heat capacities observed in PVD glasses.[1,19] Interestingly, we observe suppression of the secondary relaxation amplitude even at temperatures where the reversing heat capacities of the vapor-deposited glasses are approaching the value observed in liquid-cooled glasses.[25] The reason for this lack of correlation at low deposition temperatures is an open and intriguing question.

B. Estimation of the structural relaxation time deep in the glassy state

Measurements of the structural relaxation time in the glassy state provide key information about the size of barriers in the potential energy landscape and may be useful for testing theories of glassy dynamics that predict diverging time scales at nonzero temperatures. One of the most common descriptions of supercooled liquid dynamics is the Vogel-Fulcher-Tammann (VFT) equation,

$$\log \tau_\alpha = A + \frac{B}{T - T_0}. \tag{3}$$

Here, A is a prefactor, B is analogous to the activation energy in an Arrhenius expression, T is temperature, and T_0 is the temperature at which τ_α diverges to infinity. A point of contention regarding the VFT equation is its ability to predict equilibrium structural relaxation times at low temperatures, i.e., $\tau_\alpha > 100$ s. Dielectric relaxation experiments on poly(vinylacetate) indicate that the VFT equation provides an accurate description of supercooled liquid dynamics even as τ_α approaches 10^8 s.[33] However, as the VFT equation cannot often describe the entire dynamic range from 10^{-12} s to 10^2 s with a single set of parameters, the applicability of the equation at low temperatures is open to question.[34] A feature of the VFT equation is the implication of a diverging relaxation time at T_0. It has been reported that models which do not include a diverging time scale are equally able to describe experimental data for a number of supercooled liquids.[35,36] Naturally, given the interest in equilibrium relaxation times at temperatures below the conventional T_g, there have been a number of proposals for how to obtain these times.[16,37–39] More generally, it is of interest to understand the relaxation time of any glass that is deep in the potential energy landscape.

Here, we use the suppression of the secondary relaxation in vapor-deposited glasses of MMT, in combination with aging data acquired on liquid-cooled samples, to estimate the structural relaxation times (τ_α) of the vapor-deposited samples. This procedure, which is closely related to the work in Refs. 40–42, makes use of the observation that the secondary relaxation amplitude has been observed empirically to decrease linearly with the logarithm of the aging time, as shown for MMT in Figs. 5(b) and 5(c). For example, during the isothermal aging of a liquid-cooled glass of toluene at 0.94 T_g (110 K), the β peak amplitude was observed to decrease linearly vs log(time) for 210 h.[19] We assume that the amplitude of the secondary relaxation stops evolving when the sample ages to equilibrium. This is consistent with previous experimental work,[40] quantitative models,[2] and with the data shown in Fig. 5(a). In support of this assumption, in the supplementary material, we show that the high frequency wing of the α relaxation stops evolving at the same aging time as does the amplitude of the secondary relaxation, for the experiment shown in Fig. 5(a). We identify the aging time when equilibrium is achieved as the structural relaxation time (τ_α); in Fig. 5(a), we approximate this by the intersection between the two lines shown. Using this approach, we find $\tau_\alpha \approx 10^{4.4}$ s for the liquid-cooled glass.

For the vapor-deposited glasses, we use the observed suppression of the secondary relaxation to identify τ_α in a manner similar to

that described in the previous paragraph. For example, in Fig. 5(b), we see that the vapor-deposited glass has the secondary relaxation amplitude expected after $\approx 10^{6.6}$ s of aging at 0.92 T_g (156 K). We adopt this as our estimate for τ_α for this sample. To make our analysis clear, we consider two scenarios. If the vapor-deposited glass has the properties of the supercooled liquid at the deposition temperature, then we estimate τ_α for the supercooled liquid by this procedure, analogous to Fig. 5(a). If the equilibrium supercooled liquid at the deposition temperature were to exhibit an even greater reduction of the secondary relaxation amplitude than that observed for the vapor-deposited glass, then this procedure estimates a nonequilibrium τ_α that characterizes structural relaxation in the nonequilibrium vapor deposited glass. This last conclusion follows from the assumption of "normal aging," i.e., the regime where the nonequilibrium τ_α is similar to the aging time.[43,44] Previous work has more precisely defined a nonequilibrium relaxation time.[45]

Figure 7 shows a relaxation map for MMT that includes data for the supercooled liquid, liquid-cooled glasses, and vapor-deposited glasses. τ_α values for the supercooled liquid and liquid-cooled glasses were obtained by fitting Eq. (1) to the experimental data. Chen *et al.* measured the dielectric relaxation of the supercooled liquid of MMT,[24] and the dashed line in Fig. 7 shows its fit to the VFT equation including an extrapolation to low temperature. The estimated values of τ_α for the vapor-deposited glasses, obtained as shown in Fig. 5, are also shown in the figure. The value of τ_α estimated for deposition at 0.96 T_g (163 K) [Fig. 5(a)] is consistent with the extrapolated VFT dependence. On the other hand, samples deposited at 0.92 T_g (156 K) and 0.86 T_g (146 K) have estimated relaxation times that are approximately 1.5 and 4.8 decades shorter, respectively, than the structural relaxation time predicted by the extrapolated VFT fit.

Figure 7 indicates that the vapor-deposited glasses have estimated τ_α values that are 1–5 orders of magnitude longer than those of a glass at the same temperature prepared by cooling the liquid. This is qualitatively consistent with the observed kinetic stability of these glasses. If we were certain that the PVD glasses were deposited in the limit of low deposition rates, we could conclude from Fig. 7 that the extrapolated VFT equation is not applicable far below the conventional T_g. Since we do not know that this is the case, we regard the estimated τ_α values for PVD glasses shown in Fig. 7 as lower bounds for the equilibrium supercooled liquid.

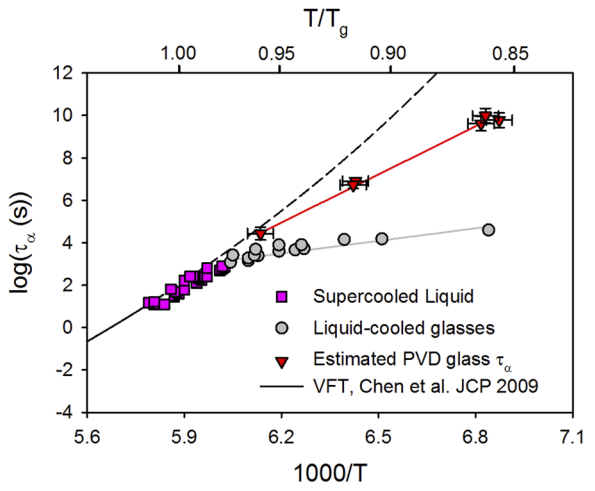

FIG. 7. Relaxation diagram for MMT. Supercooled liquid and liquid-cooled glass values obtained from the fit parameters of Eq. (1). PVD glass τ_α estimated from extrapolated aging data. Solid lines are guides to the eye. The VFT equation from Ref. 24 is shown as a dashed line for comparison. Vertical error bars have the same meaning as the horizontal error bars in Fig. 5. Horizontal error bars represent a temperature uncertainty of ±1 K.

In making the statements in the previous paragraph, we rely on the assumptions stated above for determining τ_α values for the PVD glasses. Given that we estimate τ_α values approaching 10^{10} s (≈300 years) based upon measurements that take place in roughly one day, it is not surprising that important assumptions are needed. Previous efforts to extract extremely large values of τ_α have also involved significant assumptions, e.g., the applicability of time-aging time superposition[35,39,46] or the use of a relationship between two properties in a regime where it cannot be directly tested.[38]

V. CONCLUSION

In this work, we use *in situ* dielectric relaxation spectroscopy to characterize the suppression of excess wing relaxations in vapor-deposited MMT glasses. At the optimal deposition conditions, MMT's secondary relaxation can be suppressed by 70% relative to a liquid-cooled glass, which is similar to other recently studied systems as shown in Fig. 1. The suppression of the secondary relaxation is found to have the same dependence on deposition temperature as kinetic stability. We have shown that the excess wing relaxation of MMT can be understood as a submerged β peak. We anticipate that PVD could be used to improve the resolution of overlapping peaks in dielectric loss spectra of other glass forming systems.

We have utilized the secondary relaxation suppression to estimate the structural relaxation time of PVD glasses of MMT. Extrapolations of the aging behavior of liquid-cooled glasses were used to estimate the structural relaxation times of PVD glasses deposited at temperatures as low as 0.86 T_g (146 K). The estimated α relaxation times for the PVD glasses exceeded those of liquid-cooled glasses (at the same temperature) by as much as 5 orders of magnitude. The temperature dependence of the estimated τ_α for these particular glasses is considerably weaker than that predicted by VFT extrapolation from the supercooled liquid, but it is possible that a steeper temperature dependence would be observed for glasses produced in the limit of a low deposition rate. It would be useful to compare this method of estimating the structural relaxation time for PVD glasses to other proposals in the literature.

SUPPLEMENTARY MATERIAL

See the supplementary material for comparisons of kinetic stability results to previous AC nanocalorimetry results, versions of Fig. 6 that distinguish deposition rates, and evolution of the τ_{HN} parameter with the aging time for a liquid-cooled MMT glass aged at 0.96 T_g (163 K).

ACKNOWLEDGMENTS

We thank the U.S. National Science Foundation (Grant Nos. CHE-1564663 and CHE-1854930) for supporting this work.

REFERENCES

[1] M. Goldstein, J. Chem. Phys. **64**(11), 4767–4774 (1976).
[2] J. C. Dyre and N. B. Olsen, Phys. Rev. Lett. **91**(15), 155703 (2003).
[3] P. G. Debenedetti and F. H. Stillinger, Nature **410**(6825), 259–267 (2001).
[4] K. L. Ngai and M. Paluch, J. Phys. Chem. B **107**(28), 6865–6872 (2003).
[5] E. O. Kissi, H. Grohganz, K. Lobmann, M. T. Ruggiero, J. A. Zeitler, and T. Rades, J. Phys. Chem. B **122**(10), 2803–2808 (2018).
[6] W. D. Oliver and P. B. Welander, MRS Bull. **38**(10), 816–825 (2013).
[7] A. Kudlik, S. Benkhof, T. Blochowicz, C. Tschirwitz, and E. Rössler, J. Mol. Struct. **479**(2-3), 201–218 (1999).
[8] S. Hensel-Bielowka and M. Paluch, Phys. Rev. Lett. **89**(2), 025704 (2002).
[9] U. Schneider, R. Brand, P. Lunkenheimer, and A. Loidl, Phys. Rev. Lett. **84**(24), 5560–5563 (2000).
[10] P. Lunkenheimer, R. Wehn, T. Riegger, and A. Loidl, J. Non-Cryst. Solids **307-310**, 336–344 (2002).
[11] K. L. Ngai and M. Paluch, J. Chem. Phys. **120**(2), 857–873 (2004).
[12] G. P. Johari and M. Goldstein, J. Chem. Phys. **53**(6), 2372–2388 (1970).
[13] M. Vogel and E. Rössler, J. Chem. Phys. **114**(13), 5802–5815 (2001).
[14] M. Vogel and E. Rössler, J. Chem. Phys. **115**(23), 10883–10891 (2001).
[15] C. W. Brian and L. Yu, J. Phys. Chem. A **117**(50), 13303–13309 (2013).
[16] M. D. Ediger, J. Chem. Phys. **147**(21), 210901 (2017).
[17] S. F. Swallen, K. L. Kearns, M. K. Mapes, Y. S. Kim, R. J. McMahon, M. D. Ediger, T. Wu, L. Yu, and S. Satija, Science **315**(5810), 353–356 (2007).
[18] S. S. Dalal, Z. Fakhraai, and M. D. Ediger, J. Phys. Chem. B **117**(49), 15415–15425 (2013).
[19] H. B. Yu, M. Tylinski, A. Guiseppi-Elie, M. D. Ediger, and R. Richert, Phys. Rev. Lett. **115**(18), 185501 (2015).
[20] C. Rodriguez-Tinoco, M. Rams-Baron, K. L. Ngai, K. Jurkiewicz, J. Rodriguez-Viejo, and M. Paluch, Phys. Chem. Chem. Phys. **20**(6), 3939–3945 (2018).
[21] C. Rodríguez-Tinoco, K. L. Ngai, M. Rams-Baron, J. Rodriguez-Viejo, and M. Paluch, Phys. Chem. Chem. Phys. **20**(34), 21925–21933 (2018).
[22] B. Riechers, A. Guiseppi-Elie, M. D. Ediger, and R. Richert, J. Chem. Phys. **150**(21), 214502 (2019).
[23] K. L. Ngai, M. Paluch, and C. Rodriguez-Tinoco, Phys. Chem. Chem. Phys. **20**(43), 27342–27349 (2018).
[24] Z. Chen, Y. Zhao, and L. M. Wang, J. Chem. Phys. **130**(20), 204515 (2009).
[25] M. Tylinski, A. Sepulveda, D. M. Walters, Y. Z. Chua, C. Schick, and M. D. Ediger, J. Chem. Phys. **143**(24), 244509 (2015).
[26] A. Sepulveda, M. Tylinski, A. Guiseppi-Elie, R. Richert, and M. D. Ediger, Phys. Rev. Lett. **113**(4), 045901 (2014).
[27] Z. Chen, A. Sepúlveda, M. D. Ediger, and R. Richert, Eur. Phys. J. B **85**(8), 268 (2012).
[28] K. L. Kearns, S. F. Swallen, M. D. Ediger, T. Wu, Y. Sun, and L. Yu, J. Phys. Chem. B **112**(16), 4934–4942 (2008).
[29] S. L. Ramos, M. Oguni, K. Ishii, and H. Nakayama, J. Phys. Chem. B **115**(49), 14327–14332 (2011).
[30] M. S. Beasley, C. Bishop, B. J. Kasting, and M. D. Ediger, J. Phys. Chem. Lett. **10**, 4069–4075 (2019).
[31] E. Leon-Gutierrez, A. Sepulveda, G. Garcia, M. T. Clavaguera-Mora, and J. Rodriguez-Viejo, Phys. Chem. Chem. Phys. **18**(11), 8244–8245 (2016).
[32] S. S. Dalal, D. M. Walters, I. Lyubimov, J. J. de Pablo, and M. D. Ediger, Proc. Natl. Acad. Sci. U. S. A. **112**(14), 4227–4232 (2015).
[33] R. Richert, Physica A **287**(1-2), 26–36 (2000).
[34] C. A. Angell, K. L. Ngai, G. B. McKenna, P. F. McMillan, and S. W. Martin, J. Appl. Phys. **88**(6), 3113–3157 (2000).
[35] J. Zhao, S. L. Simon, and G. B. McKenna, Nat. Commun. **4**, 1783 (2013).
[36] T. Hecksher, A. I. Nielsen, N. B. Olsen, and J. C. Dyre, Nat. Phys. **4**(9), 737–741 (2008).
[37] G. B. McKenna and S. L. Simon, Macromolecules **50**(17), 6333–6361 (2017).
[38] E. A. Pogna, C. Rodriguez-Tinoco, G. Cerullo, C. Ferrante, J. Rodriguez-Viejo, and T. Scopigno, Proc. Natl. Acad. Sci. U. S. A. **112**(8), 2331–2336 (2015).
[39] H. Yoon and G. B. McKenna, Sci. Adv. **4**(12), eaau5423 (2018).
[40] H. Yardimci and R. L. Leheny, J. Chem. Phys. **124**(21), 214503 (2006).
[41] R. Casalini and C. M. Roland, Phys. Rev. Lett. **102**(3), 035701 (2009).
[42] P. Lunkenheimer, R. Wehn, U. Schneider, and A. Loidl, Phys. Rev. Lett. **95**(5), 055702 (2005).
[43] M. Warren and J. Rottler, Phys. Rev. Lett. **110**(2), 025501 (2013).
[44] L. C. E. Struik, *Physical Aging in Amorphous Polymers and Other Materials* (Elsevier Scientific, New York, 1977).
[45] K. Niss, Phys. Rev. Lett. **119**(11), 115703 (2017).
[46] G. B. McKenna and J. Zhao, J. Non-Cryst. Solids **407**, 3–13 (2015).